Clinical Imaging 55 (2019) 76–82

Contents lists available at ScienceDirect

Clinical Imaging

journal homepage: www.elsevier.com/locate/clinimag

Neuroradiology

Application of diffusion-weighted MR imaging with ADC measurement for distinguishing between the histopathological types of sinonasal neoplasms

Mehmet Gencturk[a], Kerem Ozturk[a], Emiro Caicedo-Granados[b], Faqian Li[c], Zuzan Cayci[a,*]

[a] Department of Radiology, University of Minnesota Medical Center, Minneapolis, MN, USA
[b] Department of Otolaryngology-Head and Neck Surgery, University of Minnesota Medical Center, Minneapolis, MN, USA
[c] Department of Pathology and Laboratory Medicine, University of Minnesota Medical Center, Minneapolis, MN, USA

ARTICLE INFO

Keywords:
Sinonasal neoplasm
Magnetic resonance imaging (MRI)
Diffusion-weighted imaging (DWI)
Squamous cell carcinoma
Apparent diffusion coefficient (ADC)

ABSTRACT

Purpose: To evaluate the potential contribution of quantitative DWI parameters including ADC_{mean} and ADC_{ratio} values to help in distinguishing the histopathological types of sinonasal neoplasms.

Methods: This retrospective study included 83 patients (50 males, 33 females; mean age 61 years) with pathologically proven untreated sinonasal neoplasms who have undergone diffusion-weighted MRI imaging from February 2010 to August 2017. Diffusion-weighted MRI was performed on a 3 T unit with b factors of 0 and 1000 s/mm^2, and ADC maps were generated. Mean ADC values of sinonasal tumors and ADC ratios (ADC_{mean} of the tumor to ADC_{mean} of pterygoid muscles) were compared with the histopathological diagnosis by utilizing the Kruskal-Wallis non-parametric test.

Results: Mean ADC_{mean} and ADC_{ratio} were 0.8 (SD, ± 0.4) × (10^{-3} mm^2/s) and 1.2 (SD, ± 0.5), respectively, and each parameter was significantly different between histopathological types ($p < 0.05$). Mean ADC_{mean} and ADC_{ratio} were higher in adenoid cystic carcinoma (ACC) than in SCC, lymphoma, neuroendocrine carcinoma and sinonasal undifferentiated carcinoma (SNUC) ($p < 0.05$). Optimized ADC_{mean} thresholds of 0.79, 0.81, 0.74 and 0.78 (10^{-3} mm^2/s) achieved maximal discriminatory accuracies of 100%, 79%, 100% and 89% for ACC/SNUC, ACC/SCC, ACC/neuroendocrine carcinoma, and ACC/lymphoma, respectively.

Conclusions: The optimized ADC_{mean} threshold of 0.80 (10^{-3} mm^2/s) could be used to differentiate ACC from non-ACC sinonasal neoplasms with maximal discriminatory accuracy (82%) and sensitivity of 100%. However, there is considerable overlapping of the ADC_{mean} and ADC_{ratio} values among non-ACC sinonasal neoplasms hence surgical biopsy is still needed.

1. Introduction

Sinonasal malignancies are the heterogeneous group of tumors with a wide variety of biologic activity [1,2]. Since the treatment strategy for the sinonasal malignancies differs regarding the histopathological type, the development of an imaging technique that accurately identifies these features is substantial to ascertain a suitable treatment approach [3,4]. Recently, diffusion-weighted imaging (DWI) with a calculated apparent diffusion coefficient (ADC) value has been recognized as an important tool to improve the diagnosis of sinonasal tumors [5].

DWI is commonly utilized to gather information related to the cellularity and biological activity of tumors [6,7]. Because DWI is non-invasive and quick to perform, it could be utilized as an adjunct to conventional imaging in the characterization of sinonasal malignancies [8]. In the light of these data, since the various histopathological type of tumors would have different biological activities and cellularities [9], we performed this study to investigate the potential contribution of DWI in the characterization of sinonasal tumors.

Recent studies on sinonasal tumors have shown that ADC values of DWI may provide substantial information to discriminate benign from malignant sinonasal lesions as well as to identify different histopathological types of sinonasal malignancies [10]. However, information was limited for a few histopathological types only, and most studies using DWI were based on small sample size. At present, no large studies regarding ADC of sinonasal malignant tumors are available, and to our knowledge, the ADCs of adenoid cystic carcinoma, neuroendocrine carcinoma, and other rare tumors remain unknown.

Our aim was to assess the usefulness of quantitative DWI parameters including ADC_{mean} and ADC_{ratio} values to help in distinguishing the histopathological types of sinonasal neoplasms.

* Corresponding author.
E-mail addresses: genct003@umn.edu (M. Gencturk), keremozturk@uludag.edu.tr (K. Ozturk), caic0001@umn.edu (E. Caicedo-Granados), lif@umn.edu (F. Li), cayci001@umn.edu (Z. Cayci).

https://doi.org/10.1016/j.clinimag.2019.02.004
Received 4 September 2018; Received in revised form 20 January 2019; Accepted 6 February 2019

2. Materials and methods

2.1. Subjects

This retrospective study was approved by our hospital's institutional review board and conducted in compliance with the Health Insurance Portability and Accountability Act guidelines.

Electronic medical and imaging records of patients diagnosed with sinonasal malignant lesions at the University of Minnesota Medical Center (M-Health) between February 2010 and August 2017 were analyzed, and 93 patients with tumors in the sinonasal region who underwent pretreatment head and neck MRI including DWI were identified. Total of 6 patients was not included in the study because their images revealed motion (n = 3) or susceptibility artifacts (n = 3). It was not possible to measure the ADC values of two lesions located adjacent to paranasal sinus air, because of susceptibility artifacts and susceptibility artifacts seriously affected DW images in one patient with fixed partial dentures. Tumors originating from nasal vestibule were not included (n = 1). Nasopharyngeal carcinoma (n = 1) and tumors originating from the oral cavity and extending into the paranasal sinuses (n = 2) were excluded. Therefore, the study cohort consisted of 83 patients (50 men, 33 women; mean age 61 years; age range 20–95 years).

The clinical records of patients were reviewed for demographic, radiographic, and histopathological data. Patients were staged according to American Joint Committee on Cancer criteria (AJCC) [11]; the University of California Los Angeles staging system [12] was used for olfactory neuroblastoma from documented clinical and pathologic findings.

2.2. Technique

Images were acquired on a 3 Tesla MRI scanner (Siemens MAGNETOM Trio or Siemens MAGNETOM Skyra) by using a 16-channel head coil. The sequence parameters for conventional images were as follows; T1WI (TR, 450–600 ms; TE, 12 ms; matrix size, 288 × 224; field of view, 24 × 24 cm; acquisition time, 1.44 min; 1 excitation), T2WI (TR, 3000–5000 ms; TE, 90–105 ms; matrix size, 288 × 288, field of view, 24 × 24 cm; acquisition time, 2.30 min; 2 excitations), followed by contrast-enhanced, fat-saturated T1-weighted spin-echo images.

DWI was performed by using a spin-echo, single-shot echoplanar imaging (EPI) sequence (TR, 5500 ms; TE, 92 ms; section thickness of 4 mm, with an interslice gap of 1 mm; matrix size, 256 × 128; field of view, 20 × 24 cm; acquisition time, 1.44 min; 1 excitation). The resultant acquisition time varied from 1 to 2 min.

2.3. Image analysis

Interpretation of MR images was performed by a dedicated radiologist (Z.C.) with clinical experience of 10 years in head and neck imaging re-reviewed all images without knowing the final histopathological results.

The ADC measurements were performed on ADC maps which were generated from DWIs with b factors of 0 and 1000 s/mm^2 by using Philips Extended MR Workspace (version 2.6.3.2 Philips Medical Systems). Three region-of-interests (ROIs) from the solid portion of the sinonasal lesion were obtained to calculate a mean ADC value. ROIs were placed as broadly as possible while excluding necrotic or cystic portions of the tumors (Figs. 1 and 2). Three separate ROI measurements were made each in the lateral pterygoid muscles to obtain mean ADC value to validate our method by calculating the sinonasal tumor-to muscle signal intensity ratios on the ADC map (ADC_{ratio}). The size of the ROIs was kept constant by utilizing a copy-and-paste function.

DW images at b values of 0, and 1000 s/mm^2 were interpreted qualitatively to determine whether lesion demonstrate facilitated or restricted diffusion. If the lesion retained its signal intensity or showed a minimal decrease with increasing b values, it was labeled as restricted diffusion, while a decrease in signal intensity on increasing b values was regarded as facilitated diffusion. Corresponding ADC maps showed hypointense signal in lesions with restricted diffusion and hyperintense signal in those with facilitated diffusion.

2.4. Statistical analysis

Continuous variables were expressed as a mean ± standard deviation, and categorical variables were expressed as frequencies and percentages. Shapiro Wilk test was performed for the normality of the test. The Kruskal-Wallis non-parametric analysis of variance test was utilized to compare the mean ADC_{mean} and ADC_{ratio} to detect any statistically significant difference between different histopathologies and was also utilized to evaluate any correlation between the stage and the mean ADC values of sinonasal tumors. Analysis of statistical significance was performed by one-way analysis of variance (ANOVA) with posthoc Bonferroni tests for pairwise multiple comparisons of histopathological types. Diagnostic ability was calculated by receiver operating characteristic (ROC) analysis to determine ADC cutoff values to differentiate various types of sinonasal neoplasms on the basis of mean ADC_{ratio} and ADC_{mean}. The differences in the number of patients with facilitated and restricted diffusion were calculated using a x^2 or Fisher's exact test, as appropriate. The p-values < 0.05 were considered to indicate statistically significant differences. All statistical analyses were performed with commercially available software (SPSS 23.0 for Windows; SPSS Inc., Chicago, IL, USA). Data were entered into Excel spreadsheets (Microsoft, Redmond, WA).

3. Results

The mean age of the patients at the time of diagnosis was 61 years (range, 20–95 years), and a slight male predilection was noted. No significant differences with regard to the mean age or gender distribution were identified according to histopathological types ($p > 0.05$). Tumor size assessed by the longest diameter measured in the axial plane on MRI according to RECIST criteria was 48 ± 18 mm (range 12–97 mm). The majority of patients presented with locally advanced disease according to the AJCC and the University of California Los Angeles staging system.

As regards the histopathological results, the study group included SCC (n = 26), olfactory neuroblastomas (n = 6), adenocarcinoma (n = 2), sinonasal undifferentiated carcinoma (SNUC) (n = 7), lymphoma (n = 9), malignant melanoma (n = 5), sarcoma (n = 9), poorly differentiated carcinoma (n = 2), adenoid cystic carcinoma (n = 10), high grade neuroendocrine carcinoma (n = 4) and metastatic tumor (n = 3). Of the 9 lymphomas; 7 were diffuse large B-cell lymphoma and 2 were natural killer-cell/T-cell lymphoma. Out of the 9 sarcomas; 3 were carcinosarcoma, 3 were alveolar rhabdomyosarcoma, 2 were fibrosarcoma and 1 was angiosarcoma. Patient and tumor characteristics are summarized in Table 1.

3.1. DWI features

Eighty-three patients with documented numerical values had a mean ADC_{mean} and ADC_{ratio} of 0.8 (SD, ± 0.4; range, 0.04–2.2) × (10^{-3} mm^2/s) and 1.2 (SD, ± 0.5; range, 0.2–3), respectively.

The overall population was heterogeneous in terms of histopathological, and Table 2 shows the mean ADC values according to the different histopathology of sinonasal neoplasms. The ADC_{mean} and ADC_{ratio} values were significantly different between tumor types according to the Kruskal-Wallis non-parametric test ($p = 0.002$, $p < 0.001$), respectively.

The mean ADC_{mean} and ADC_{ratio} values were not statistically different between various stages ($p > 0.05$) (Fig. 3).

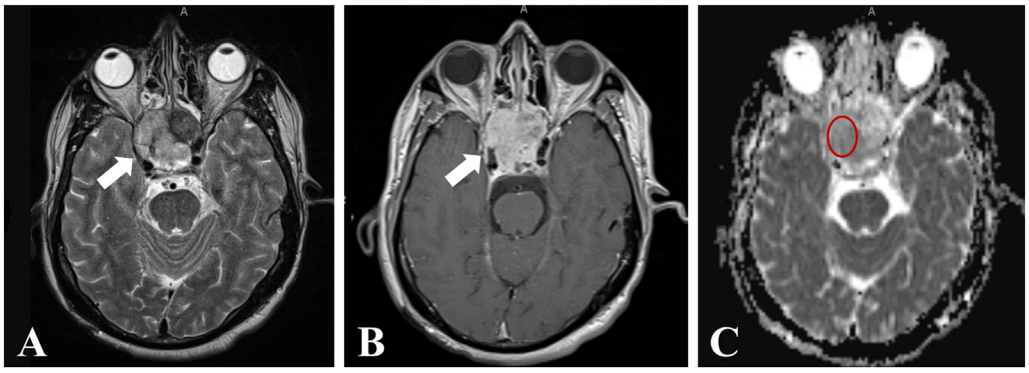

Fig. 1. Adenoid cystic carcinoma. A. Axial T2-weighted image demonstrates a mass (arrow) with intermediate signal intensity in the sphenoid sinus. B. Axial contrast enhanced T1-weighted image shows marked contrast enhancement (arrow). C. Axial ADC map demonstrates a high ADC_{mean} value in the mass ($1.38 \times 10^{-3}\,mm^2/s$) (Red ROI) denoting facilitated diffusion. (For interpretation of the references to color in this figure legend, the reader is referred to the web version of this article.)

Total of 14 lesions demonstrated facilitated diffusion, while 69 lesions revealed restricted diffusion on DW images and ADC maps. The qualitative analysis of SIs could not distinguish between the different histopathological type of sinonasal malignancies.

Among all significant ADC_{mean} and ADC_{ratio} cut-off values in the differentiation of sinonasal tumor types, the diagnostic ability of ADCs to differentiate sinonasal ACCs from different types of carcinomas provided the best discriminatory classification ($p < 0.05$).

3.2. Comparison according to ADC_{mean}

Mean ADC_{mean} was higher in ACC (1.28 ± 0.44) $\times$ ($10^{-3}\,mm^2/s$) patients than in SNUC (0.47 ± 0.3) $\times$ ($10^{-3}\,mm^2/s$) ($p = 0.001$), SCC (0.76 ± 0.38) $\times$ ($10^{-3}\,mm^2/s$) ($p = 0.017$), neuroendocrine carcinoma (0.45 ± 0.29) $\times$ ($10^{-3}\,mm^2/s$) ($p = 0.017$) and lymphoma (0.61 ± 0.44) $\times$ ($10^{-3}\,mm^2/s$) ($p = 0.009$) (Fig. 4).

Using ROC curve analysis, optimized ADC_{mean} thresholds of 0.79, 0.81, 0.74 and 0.78 ($10^{-3}\,mm^2/s$) achieved maximal discriminatory accuracies of 100%, 79%, 100% and 89% for ACC/SNUC, ACC/SCC, ACC/neuroendocrine carcinoma, and ACC/lymphoma, respectively.

When sinonasal neoplasms were divided into ACC and non-ACC groups, the optimized ADC_{mean} threshold of 0.80 ($10^{-3}\,mm^2/s$) achieved maximal discriminatory accuracy (82%) with sensitivity and specificity of 100% and 66%, respectively (Fig. 5).

3.3. Comparison according to ADC_{ratio}

Mean ADC_{ratio} was higher in ACC (1.8 ± 0.5) patients than in SNUC (0.8 ± 0.2) ($p = 0.003$), SCC (1.1 ± 0.4) ($p = 0.005$), neuroendocrine carcinoma (0.7 ± 0.1) ($p = 0.008$) and lymphoma (1.0 ± 0.4) ($p = 0.019$) (Fig. 6).

Using ROC curve analysis, optimized ADC_{ratio} thresholds of 1.22, 1.29, 0.99 and 1.21 achieved maximal discriminatory accuracies of 94%, 83%, 100% and 84% for ACC/SNUC, ACC/SCC, ACC/neuroendocrine carcinoma, and ACC/lymphoma, respectively.

When sinonasal neoplasms were divided into ACC and non-ACC groups, the optimized ADC_{ratio} threshold of 1.31 achieved maximal discriminatory accuracy (84%) with sensitivity and specificity of 90%

Table 1
Patients and tumors characteristics.

Characteristics	No. of patients	%
Sex		
Male	50	60.2
Female	33	39.8
Mean age, y	61 (Range = 20–95)	
Mean diameter, mm	50 (Range = 11–92)	
American Joint Committee on Cancer Stage		
I	6	7.2
II	18	21.7
III	25	30.1
IV	34	41
Primary sites		
Nasal cavity	40	48.2
Maxillary sinus	28	33.7
Ethmoid sinus	7	8.5
Sphenoid sinus	6	7.2
Frontal sinus	2	2.4
Histological type		
Squamous cell carcinoma	26	31.3
Adenoid cystic carcinoma	10	12
Malignant melanoma	5	6
Olfactory neuroblastoma	6	7.2
Sinonasal undifferentiated carcinoma	7	8.5
Neuroendocrine carcinoma	4	4.8
Adenocarcinoma	2	2.4
Metastatic tumor	3	3.6
Poorly differentiated carcinoma	2	2.4
Rhabdomyosarcoma	9	10.9
Lymphoma	9	10.9

Abbreviations: No., number; mm, millimeter.

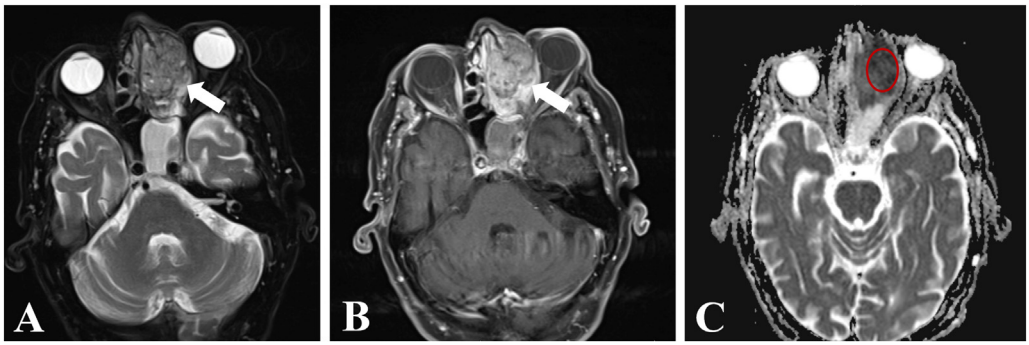

Fig. 2. Sinonasal malignant melanoma. A. Axial T2-weighted image demonstrates a mass (arrow) with iso- to hypointense signal intensity in the ethmoid air cells associated with retained secretions in the sphenoid sinus. B. Axial contrast enhanced T1-weighted image shows marked contrast enhancement (arrow). C. Axial ADC map demonstrates a low ADC_{mean} value in the mass ($0.52 \times 10^{-3}\,mm^2/s$) (Red ROI) denoting restricted diffusion and a high ADC_{mean} value in the retained fluid. (For interpretation of the references to color in this figure legend, the reader is referred to the web version of this article.)

Table 2
Mean ADC_{mean} and ADC_{ratio} according to sinonasal tumor histopathology. ADC values with bold characters demonstrate statistically significant pairwise comparisons according to one-way ANOVA test

Histopathological type (n)	ADC_{mean} ± SD (10^{-3} mm^2/s)	ADC_{ratio} ± SD
Adenocarcinoma (n = 2)	1.12 ± 0.54	1.64 ± 0.87
Adenoid cystic carcinoma (n = 10)	**1.28 ± 0.44**	**1.80 ± 0.57**
Lymphoma (n = 9)	**0.61 ± 0.44**	**1.03 ± 0.42**
Malignant melanoma (n = 5)	0.88 ± 0.45	1.16 ± 0.56
Metastasis (n = 3)	0.77 ± 0.23	1.08 ± 0.30
Neuroendocrine carcinoma (n = 4)	**0.45 ± 0.29**	**0.75 ± 0.13**
Olfactory neuroblastoma (n = 6)	0.97 ± 0.20	1.44 ± 0.42
Poorly differentiated carcinoma (n = 2)	0.61 ± 0.01	0.83 ± 0.008
Sarcoma (n = 9)	0.76 ± 0.29	1.26 ± 0.35
Squamous cell carcinoma (n = 26)	**0.76 ± 0.38**	**1.11 ± 0.45**
SNUC (n = 7)	**0.46 ± 0.30**	**0.85 ± 0.20**
p-Value (Kruskal-Wallis Test)	0.002	0.0001

SNUC, sinonasal undifferentiated carcinoma; SD, standard deviation; n, number.
Bold characters demonstrate statistically significant pairwise comparisons ($p < 0.05$).

and 78%, respectively (Fig. 5).

4. Discussion

DWI has emerged as a powerful imaging tool for the diagnosis of various head and neck malignancies with promising outcomes [13]. DWI may offer a better characterization of tumors because it reflects the Brownian motion of water protons, quantified by using the ADC value [14]. In oncological imaging, decreased ADC may be regarded as a signal of increased cell proliferation and correlates with the cellularity of tumor tissue [15].

Recently, Razek et al. [16] demonstrated that ADC values might provide practical information to distinguish malignant from benign sinonasal lesions as well as may help to differentiate sinonasal carcinoma from sarcoma. However, none of the previous reports specifically determined ADC_{mean} and ADC_{ratio} values of different sinonasal neoplasms in a larger study population.

Our findings showed a statistically significant difference of ADC_{mean} and ADC_{ratio} parameters between the different types of sinonasal tumors. Mean ADC_{mean} and ADC_{ratio} were significantly higher in adenoid cystic carcinoma (ACC) than in SCC, lymphoma, SNUC, and neuroendocrine carcinoma. Interestingly, the mean ADC of ACC was higher than any other sinonasal tumors.

The differences in ADC values between some sinonasal tumor types may have a few possible explanations [17]. Firstly, tumors may differ systematically in terms of cellularity which is well correlated with reduced water diffusivity [18]. Lymphoma is a major example of this phenomenon due to its hypercellular nature likely explains the significantly lower ADC values [19]. Although necrotic and cystic changes in tumors (i.e., sarcoma, SNUC) [20] have been shown to enhance diffusivity on a macroscopic level, we believe that these factors had minimal impact in our study because they were excluded in ROIs as possible. Small cystic areas in the tumor have been shown to produce a speckled diffusion pattern on DWI and may explain the higher observed ADC values in the sinonasal adenoid cystic carcinomas [21].

Some other histopathological features can have a substantial impact on ADC values. The diffusivity of water molecules can be restricted by keratinous debris in the tumor [22]. In our series, SCCs had low ADC values, implying that these tumors can potentially have keratinous debris within the hypercellular tumoral structure. In our series, SNUCs and neuroendocrine carcinoma demonstrated the lowest mean ADC values, possibly due to their characteristic histopathological pattern which reveals small malignant cells with little cytoplasmic space for random movement of water molecules [23].

We recognized no difference between malignant melanoma, poorly differentiated carcinoma, metastasis, sarcoma, olfactory neuroblastoma, and adenocarcinoma on DWI regarding the quantitative ADC measurement. This was likely due to the comparatively small number of cases and due to the fact that the ADC ranges overlap in each tumor type. Further studies are necessary because our series contained only

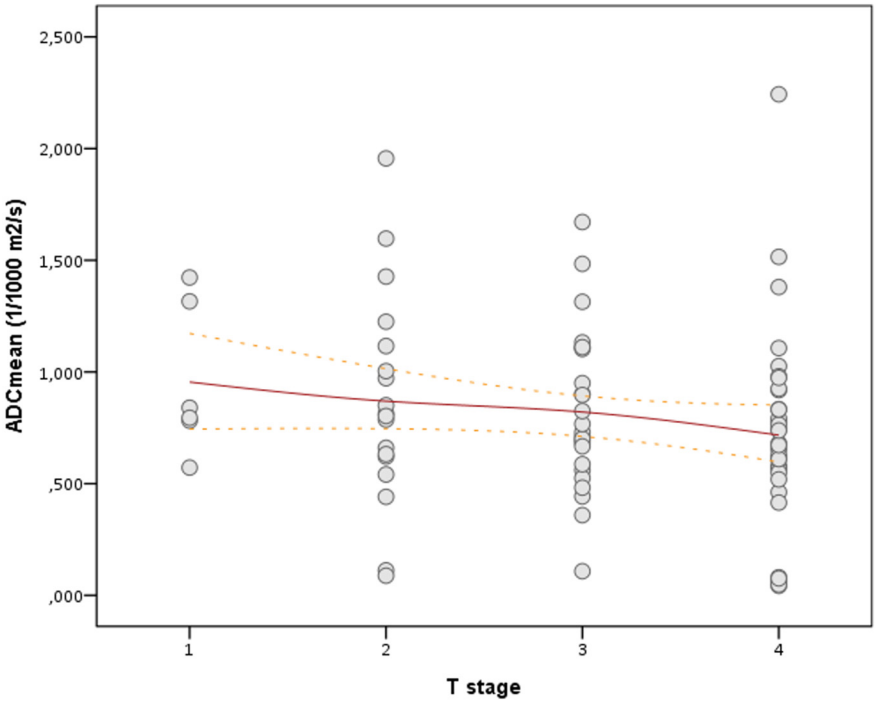

Fig. 3. Scatterplot demonstrates the result of analysis of variance test between ADC_{mean} and T stages of sinonasal neoplasms. Correlation is not significant. The best fit-line is shown as solid line, curves above and below best fit-line represent upper and lower bounds of 95% confidence interval.

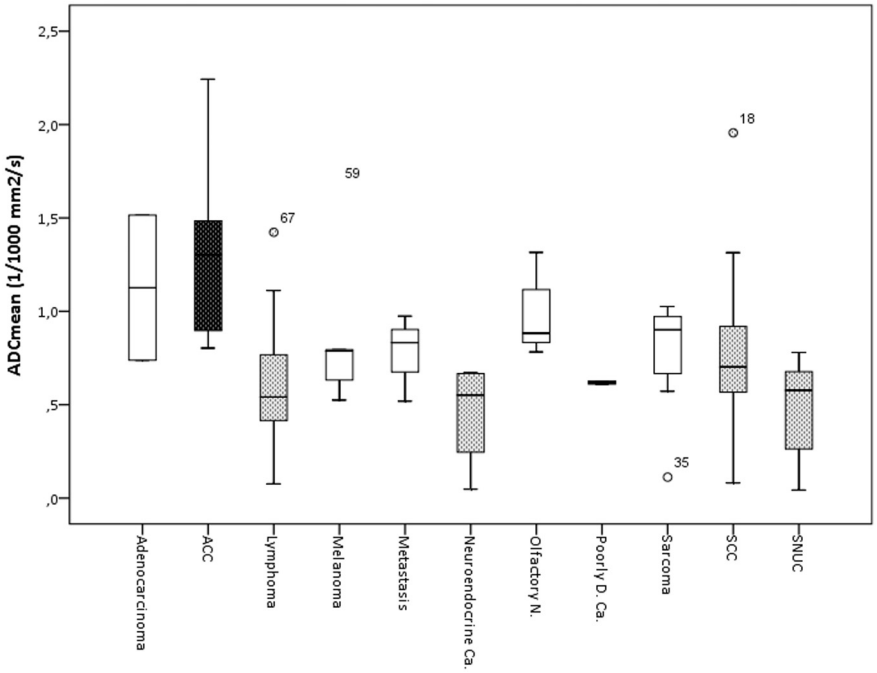

Fig. 4. Box plot shows mean ADC_{mean} values and range. (ACC, adenoid cystic carcinoma; Neuroendocrine Ca., neuroendocrine carcinoma; Olfactory N., olfactory neuroblastoma; Poorly D. Ca., poorly differentiated carcinoma; SCC, squamous cell carcinoma; SNUC, sinonasal undifferentiated carcinoma) (error bars represent the ± SD).

two cases of adenocarcinoma and poorly differentiated carcinoma.

Our results were in line with the previous reports that are evaluating the sinonasal neoplasms with DWI. In a study by Razek et al. [16], a significant difference in ADC values between sinonasal carcinoma and sarcoma as well as between well and poorly differentiated sinonasal tumors were reported. The mean ADC values of SNUCs were significantly lower than the most of other sinonasal tumor types in our study. These results conflicted with a study by Sasaki et al. [24] which demonstrated a significant lower overall ADC values for sinonasal lymphomas than for SNUCs. On the other hand, we could only find one report of the radiologic features of the sinonasal sarcomas in the literature. Wang et al. [25] found a statistically significant difference in ADC between adult rhabdomyosarcoma and carcinomas. The lower ADC of rhabdomyosarcoma was linked with the tumor structure including a large number of undifferentiated cells with minimal cytoplasm. Nevertheless, we could not identify any statistical significance between sarcoma and carcinomas in regard to DWI evaluation in our study. Das et al. [26] studied a total of 18 pathologically proven malignant lesion and found significant differences between the mean ADC value of lymphoma, adenocarcinoma and adenoid cystic carcinoma. Olfactory neuroblastoma was found to have the lowest mean ADC value, in contrast with chondrosarcoma having the highest mean ADC value.

In the current study, the majority of sinonasal neoplasms were staged as T3 and T4. This may be related to the delayed presentation, or because MR studies were possibly only obtained for the advanced stage cases due to treating physician's discretion. Large tumors are usually associated with micro- or macrocytic areas that may be associated with

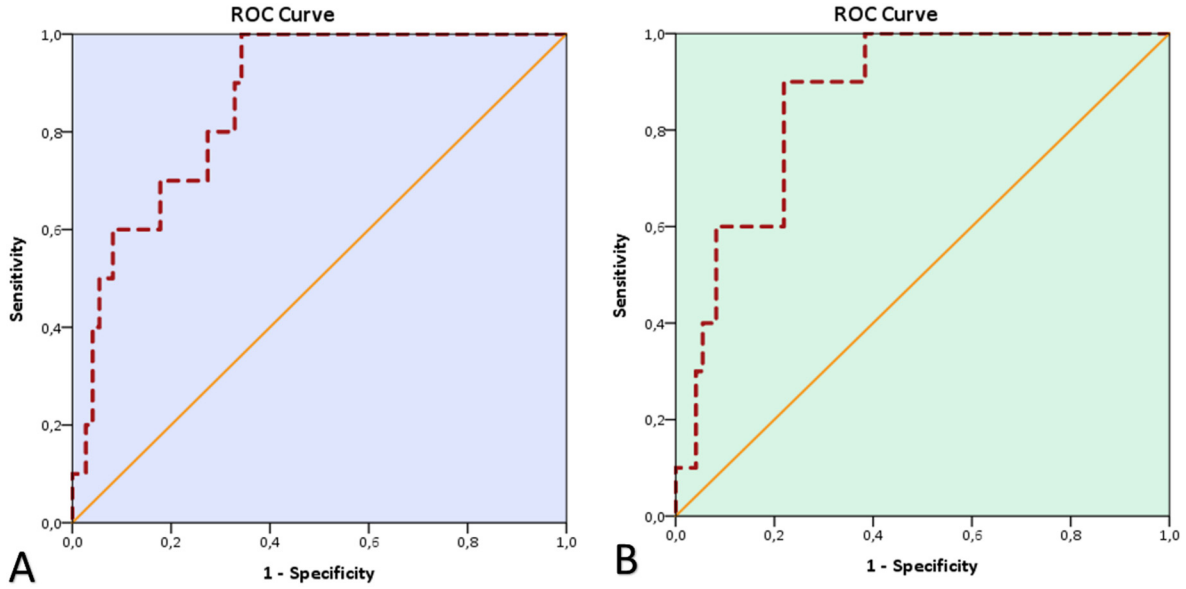

Fig. 5. Receiver operating characteristic (ROC) curve. A. The cutoff ADC_{mean} value was used to differentiate ACCs from non-ACCs was 0.80 (10^{-3} mm^2/s). The AUC was 0.86 with 100% sensitivity, 66% specificity, and 82% accuracy. B. The cutoff ADC_{ratio} value was used to differentiate ACCs from non-ACCs was 1.31. The AUC was 0.87 with 90% sensitivity, 78% specificity, and 84% accuracy.

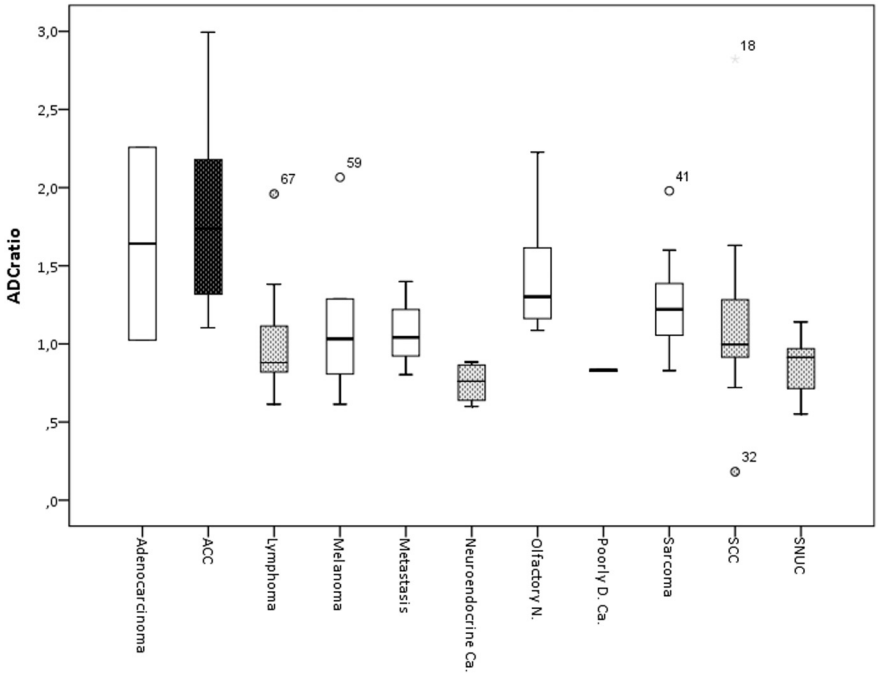

Fig. 6. Box plot shows mean ADC_{ratio} values and range. (ACC, adenoid cystic carcinoma; Neuroendocrine Ca., neuroendocrine carcinoma; Olfactory N., olfactory neuroblastoma; Poorly D. Ca., poorly differentiated carcinoma; SCC, squamous cell carcinoma; SNUC, sinonasal undifferentiated carcinoma) (error bars represent the ± SD).

higher ADC value. We selected the ROI from the solid part of the tumor to avoid bias from cystic or necrotic regions in this work. Our method of analysis can be performed routinely by obtaining ADC values at a PACS station with ROI measurement, without any additional post-processing.

The limitations of our study include that there was an imbalance between the number of available histopathological types including a low number of cases of adenocarcinoma (n = 2), poorly differentiated carcinoma (n = 2), and metastasis (n = 3). A second potential confounding factor is the lack of benign sinonasal lesions. Another limitation is that DWI is challenging to perform in the sinonasal region due to patient movements and susceptibility artifacts. This artifact could be greatly reduced when the tumors located in the nasal cavity, paranasal sinuses, and the adjacent skull base are relatively large. In this study, 73/83 (88%) cases had lesions with a largest diameter of > 3 cm. No case with visible susceptibility artifact was revealed in these larger sinonasal lesions. Besides, in a total of three cases with sinonasal tumors < 3 cm, imaging artifacts interfered with the analysis of diagnostic images. Future application of advanced MR technology, such as propeller and parallel imaging, may eliminate these confounding MRI artifacts in the sinonasal region and skull base [27].

In conclusion, the optimized ADC_{mean} threshold of 0.80 (10^{-3} mm^2/s) could be used to differentiate ACC from non-ACC sinonasal neoplasms with maximal discriminatory accuracy (82%) and sensitivity of 100%. We also found that there is considerable overlapping of the ADC_{mean} and ADC_{ratio} values among non-ACC sinonasal neoplasms hence surgical biopsy is still needed. Further studies comparing the ADC value, especially in benign sinonasal tumors and ACCs are recommended.

Competing interests

There are no potential competing interests.

Funding

None.

Acknowledgments

Not applicable.

Author contributions

Mehmet Gencturk: conceptualization; methodology; writing, reviewing, and editing; and funding acquisition.

Kerem Ozturk: conceptualization; methodology; writing, reviewing, and editing; and funding acquisition.

Emiro Caicedo-Granados: methodology and writing, reviewing, and editing.

Faqian Li: writing, reviewing, and editing.

Zuzan Cayci: conceptualization; methodology; writing, reviewing, and editing; and funding acquisition.

Conflict of interest

All authors of this manuscript, Mehmet Gencturk, Kerem Ozturk, Emiro Caicedo-Granados, Faqian Li, Zuzan Cayci declare that they have no conflict of interest.

Funding

None.

Ethical standards

All procedures performed were in accordance with the ethical standards of the institutional research committee and with the 1983 revised Helsinki declaration and its later amendments or comparable ethical standards.

Informed consent was not required.

References

[1] Eggesbø HB. Imaging of sinonasal tumours. Cancer Imaging 2012;12:136–52. https://doi.org/10.1102/1470-5206.2012.0015.

[2] Franchi A, Miligi L, Palomba A, Giovannetti L, Santucci M. Sinonasal carcinomas: recent advances in molecular and phenotypic characterization and their clinical implications. Crit Rev Oncol Hematol 2011;79:265–77. https://doi.org/10.1016/j.critrevonc.2010.08.002.

[3] Lango MN, Topham NS, Perlis CS, Flieder DB, Weaver MW, Turaka A, et al. Surgery in the multimodality treatment of sinonasal malignancies. Curr Probl Cancer 2010;34:304–21. https://doi.org/10.1016/j.currproblcancer.2010.07.001.

[4] Haerle SK, Gullane PJ, Witterick IJ, Zweifel C, Gentili F. Sinonasal carcinomas:

epidemiology, pathology, and management. Neurosurg Clin N Am 2013;24:39–49. https://doi.org/10.1016/j.nec.2012.08.004.
[5] Wang X, Zhang Z, Chen Q, Li J. Effectiveness of 3 T PROPELLER DUO diffusion-weighted MRI in differentiating sinonasal lymphomas and carcinomas. Clin Radiol 2014;69:1149–56. https://doi.org/10.1016/j.crad.2014.07.003.
[6] Thoeny HC. Diffusion-weighted MRI in head and neck radiology: applications in oncology. Cancer Imaging 2010;10:209–14. https://doi.org/10.1102/1470-7330.2010.0030.
[7] Jansen JF, Stambuk HE, Koutcher JA, Shukla-Dave A. Non-Gaussian analysis of diffusion-weighted MR imaging in head and neck squamous cell carcinoma: a feasibility study. AJNR Am J Neuroradiol 2010;31:741–8. https://doi.org/10.3174/ajnr.a1919.
[8] Razek AA. Diffusion-weighted magnetic resonance imaging of head and neck. J Comput Assist Tomogr 2010;34:808–15. https://doi.org/10.1097/rct.0b013e3181f01796.
[9] Srinivasan A, Mohan S, Mukherji SK. Biologic imaging of head and neck cancer: the present and the future. AJNR Am J Neuroradiol 2011;33:586–94. https://doi.org/10.3174/ajnr.a2535.
[10] White ML, Zhang Y, Robinson RA. Evaluating tumors and tumorlike lesions of the nasal cavity, the paranasal sinuses, and the adjacent skull base with diffusion-weighted MRI. J Comput Assist Tomogr 2006;30:490–5. https://doi.org/10.1097/00004728-200605000-00023.
[11] Lydiatt WM, Patel SG, O'Sullivan B, Brandwein MS, Ridge JA, Migliacci JC, et al. Head and Neck cancers—major changes in the American Joint Committee on cancer eighth edition cancer staging manual. CA Cancer J Clin 2017;67:122–37. https://doi.org/10.3322/caac.21389.
[12] Tajudeen BA, Arshi A, Suh JD, Palma-Diaz MF, Bergsneider M, Abemayor E, et al. Esthesioneuroblastoma: an update on the UCLA experience, 2002–2013. J Neurol Surg B Skull Base 2014;76:43–9. https://doi.org/10.1055/s-0034-1390011.
[13] Vandecaveye V, De Keyzer F, Dirix P, Lambrecht M, Nuyts S, Hermans R. Applications of diffusion-weighted magnetic resonance imaging in head and neck squamous cell carcinoma. Neuroradiology 2010;52:773–84. https://doi.org/10.1007/s00234-010-0743-0.
[14] Kolff-Gart AS, Pouwels PJW, Noij DP, Ljumanovic R, Vandecaveye V, de Keyzer F, et al. Diffusion-weighted imaging of the head and neck in healthy subjects: reproducibility of ADC values in different MRI systems and repeat sessions. AJNR Am J Neuroradiol 2014;36:384–90. https://doi.org/10.3174/ajnr.a4114.
[15] Driessen JP, van Kempen PMW, van der Heijden GJ, Philippens MEP, Pameijer FA, Stegeman I, et al. Diffusion-weighted imaging in head and neck squamous cell carcinomas: a systematic review. Head Neck 2014;37:440–8. https://doi.org/10.1002/hed.23575.
[16] Razek AA, Sieza S, Maha B. Assessment of nasal and paranasal sinus masses by diffusion-weighted MR imaging. J Neuroradiol 2009;36:206–11. https://doi.org/10.1016/j.neurad.2009.06.001.
[17] Schafer J, Srinivasan A, Mukherji S. Diffusion magnetic resonance imaging in the head and neck. Magn Reson Imaging Clin N Am 2011;19:55–67. https://doi.org/10.1016/j.mric.2010.10.002.
[18] Yun TJ, Kim JH, Kim KH, Sohn CH, Park SW. Head and neck squamous cell carcinoma: differentiation of histologic grade with standard-and high-b-value diffusion-weighted MRI. Head Neck 2012;35:626–31. https://doi.org/10.1002/hed.23008.
[19] Fong D, Bhatia KS, Yeung D, King AD. Diagnostic accuracy of diffusion-weighted MR imaging for nasopharyngeal carcinoma, head and neck lymphoma and squamous cell carcinoma at the primary site. Oral Oncol 2010;46:603–6. https://doi.org/10.1016/j.oraloncology.2010.05.004.
[20] Slootweg PJ, Ferlito A, Cardesa A, Thompson LDR, Hunt JL, Strojan P, et al. Sinonasal tumors: a clinicopathologic update of selected tumors. Eur Arch Otorhinolaryngol 2012;270:5–20. https://doi.org/10.1007/s00405-012-2025-4.
[21] Eida S, Sumi M, Sakihama N, Takahashi H, Nakamura T. Apparent diffusion coefficient mapping of salivary gland tumors: prediction of the benignancy and malignancy. AJNR Am J Neuroradiol 2007;28:116–21.
[22] Hakyemez B, Aksoy U, Yildiz H, Ergin N. Intracranial epidermoid cysts: diffusion-weighted, FLAIR and conventional MR findings. Eur J Radiol 2005;54:214–20. https://doi.org/10.1016/j.ejrad.2004.06.018.
[23] Bridge JA, Bowen JM, Smith RB. The small round blue cell tumors of the sinonasal area. Head Neck Pathol 2010;4:84–93. https://doi.org/10.1007/s12105-009-0158-6.
[24] Sasaki M, Eida S, Sumi M, Nakamura T. Apparent diffusion coefficient mapping for sinonasal diseases: differentiation of benign and malignant lesions. AJNR Am J Neuroradiol 2011;32:1100–6. https://doi.org/10.3174/ajnr.a2434.
[25] Wang X, Song L, Chong V, Wang Y, Li J, Xian J. Multiparametric MRI findings of sinonasal rhabdomyosarcoma in adults with comparison to carcinoma. J Magn Reson Imaging 2016;45:998–1004. https://doi.org/10.1002/jmri.25484.
[26] Das A, Bhalla AS, Sharma R, Kumar A, Thakar A, Sreenivas V, et al. Can diffusion weighted imaging aid in differentiating benign from malignant sinonasal masses?: a useful adjunct. Pol J Radiol 2017;82:345–55. https://doi.org/10.12659/pjr.900633.
[27] Chen X, Xian J, Wang X, Wang Y, Zhang Z, Guo J, et al. Role of periodically rotated overlapping parallel lines with enhanced reconstruction diffusion-weighted imaging in correcting distortion and evaluating head and neck masses using 3 T MRI. Clin Radiol 2014;69:403–9. https://doi.org/10.1016/j.crad.2013.11.011.